Int. J. Solids Structures Vol. 27, No. 7, pp. 865–883, 1991
Printed in Great Britain.

0020-7683/91 $3.00+.00
Pergamon Press plc

FATIGUE CRACK SPEED OF MATERIALS WITH LINEAR HARDENING

Y. C. Li and N. C. Huang
Department of Aerospace and Mechanical Engineering, University of Notre Dame, Notre Dame, IN 46556, U.S.A.

(*Received* 27 *September* 1989; *in revised form* 16 *April* 1990)

Abstract—This investigation deals with the steady propagation of a fatigue crack in a thin plate, subjected to cyclic tensile remote loading. The problem is analyzed according to a Dugdale model of the fracture process zone. Material stretches periodically in the fracture process zone prior to its failure. The effect of crack closure is considered in the analysis. Unlike previous work, our study is based on a constitutive relation of the linear work-hardening for material in the fracture process zone. The criterion of total accumulative plastic work is adopted for determination of the growth rate of the fatigue crack. Theoretical results thus obtained are compared with experimental data.

INTRODUCTION

Prediction of fatigue crack propagation speed under cyclic load is an important and difficult task in engineering. Several authors have made contributions to this area. For the problem of fatigue crack growth under tensile loading, Liu (1961) found the crack length increment per cycle dl/dN to be proportional to the square of the stress intensity factor range, ΔK. McClintock (1963), Rice (1965) and Weertman (1966) found that dl/dN could be expressed as the fourth power of ΔK, as proposed by Paris and Erdogan (1963) based on an experimental study. Rice (1967) pointed out the existence of a reverse plastic zone in front of a stationary crack during the unloading process. In the fatigue analysis, the reverse plastic deformation at the crack tip can also be induced by unloading. Elber (1970) in his experimental study, discovered the behavior of crack closure induced by the residual plastic stretch near the surface of the fatigue crack. Newman (1976) studied the behavior of crack closure by a finite element analysis. He employed an elastic–perfectly plastic model in his analysis and found that the transient behavior of crack closure was limited in the first few cycles of oscillation. Budiansky and Hutchinson (1978) first analyzed the steady crack closure behavior in a quasi-static plane stress problem, based on a Dugdale model of the fracture process zone with a perfectly plastic constitutive relation. Huang and Li (1989) also analyzed this problem and studied the speed of fatigue crack propagation dl/dN, based on the criterion of total accumulative plastic work. The problem of fatigue crack propagation with an in-plane shear mode deformation was analyzed by Lardner (1968), while the problem with an anti-plane shear mode was investigated by Huang (1988). A concept similar to the reverse plastic deformation was used in their study.

In this investigation, the criterion of total accumulative plastic work for material failure is employed with a modification that the effect of work-hardening of material in the fracture process zone is considered. For convenience of analysis, it is assumed that the constitutive relation in the fracture process zone can be represented by a linear, work-hardening relation between the traction on the boundary of the fracture process zone and the stretch of material prior to its failure. Theoretical results based on this model will be compared with experimental data.

ANALYSIS OF STATIONARY CRACK

Consider a plane stress problem of an infinite body containing a semi-infinite crack, subjected to periodic tensile mode deformation. The crack is located on the negative real axis, as shown in Fig. 1. The stress intensity factor K varies periodically between K_{max} and

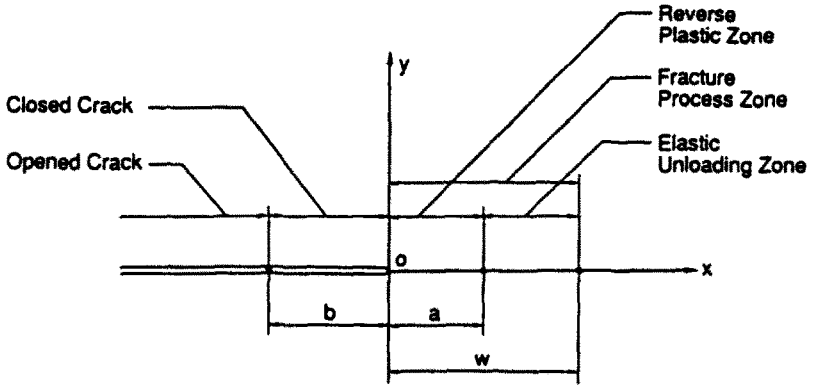

Fig. 1. Geometry of the problem for $K = K_{min} \geqslant 0$.

$K_{min} \geqslant 0$. When $K = K_{max}$ the crack is opened and there is a fracture process zone of the Dugdale type at $0 \leqslant x \leqslant w$. The analysis given here is based on the assumption of small scale yielding. The material in the fracture process zone obeys a rigid-plastic linearly-work-hardening relation

$$\sigma_y(x) = \sigma_Y + \lambda v(x), \tag{1}$$

where $\sigma_y(x)$ is the normal stress acting on the boundary of the fracture process zone, $v(x)$ is the vertical displacement on the boundary, σ_Y is the yielding stress corresponding to the residual stress for the transition from a continuum to the fracture process zone, and λ is the work-hardening parameter which is regarded as a material constant.

In the strip yielding model, the material outside of the yielding zone is elastic. According to the Dugdale model, the maximum stress intensity factor at the crack tip during loading can be expressed by

$$K_{max} = \sqrt{\frac{2}{\pi}} \int_0^w \frac{\sigma_y(x)}{\sqrt{w-x}}\, dx. \tag{2}$$

The vertical displacement of the boundary of the fracture process zone is

$$v(x) = -\frac{2}{\pi E} \int_0^w \sigma_y(t) f(t,x)\, dt + 2\sqrt{\frac{2}{\pi}} \frac{K_{max}}{E} \sqrt{w-x}, \tag{3}$$

where E is the modulus of elasticity and $f(t,x)$ is given by

$$f(t,x) = \ln \left| \frac{\sqrt{w-t} + \sqrt{w-x}}{\sqrt{w-t} - \sqrt{w-x}} \right|. \tag{4}$$

The stretch in the fracture process zone is defined by $\delta(x) = 2v(x)$.

With substitution of eqn (1) into eqn (2) and employment of the following dimensionless quantities

$$\xi = \frac{x}{w}, \quad \tau = \frac{t}{w}, \quad \Delta(\xi) = \frac{2v(x)}{\delta_0}, \quad \mu = \frac{\delta_0}{2\sigma_Y} \lambda,$$
$$\omega = \frac{2\sigma_Y^2 w}{\pi K_{max}^2}, \quad \gamma = \frac{2K_{max}^2}{\sigma_Y \delta_0 E}, \tag{5}$$

eqns (2) and (3) become

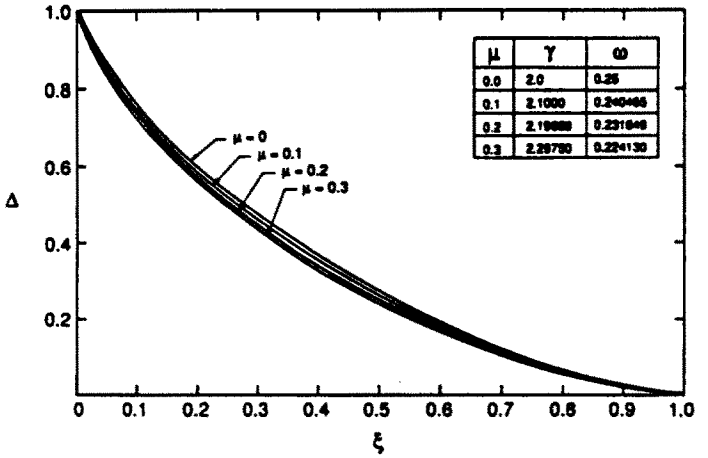

μ	γ	ω
0.0	2.0	0.25
0.1	2.1000	0.240465
0.2	2.19888	0.231848
0.3	2.29798	0.224130

Fig. 2. Crack opening displacement at $K = K_{max}$.

$$\Delta(\xi) = -\gamma\omega \int_0^1 [1+\mu\Delta(\tau)]g(\tau,\xi)\,d\tau + 2\gamma\sqrt{\omega}\sqrt{1-\xi}, \tag{6}$$

$$\omega = \left[\int_0^1 \frac{1+\mu\Delta(\xi)}{\sqrt{1-\xi}}\,d\xi\right]^{-2}, \tag{7}$$

where δ_0 is the crack opening displacement at the crack tip, i.e. $\delta_0 = \delta(0) = 2v(0)$, and

$$g(\tau,\xi) = \ln\left|\frac{\sqrt{1-\tau}+\sqrt{1-\xi}}{\sqrt{1-\tau}-\sqrt{1-\xi}}\right|. \tag{8}$$

With any fixed value of μ, $\Delta(\xi)$ can be solved by eqns (6) and (7). In the solution, the value of $\Delta(\tau)$ is expressed by a piecewise linear interpolation function of τ such that eqn (6) can be discretized into a set of linear algebraic equations, from which the value of $\Delta(\tau)$ can then be solved if γ and ω are known. With the use of the solution of $\Delta(\tau)$, the new value of ω can be determined by eqn (7). By this iterative procedure, the solution of $\Delta(\tau)$ and ω can be obtained with satisfactory accuracy. The value of γ can be determined by the condition $\Delta(0) = 1$, which involves another iterative process. The numerical results for $\mu = 0.1$, 0.2 and 0.3 are shown in Fig. 2. The values of γ and ω for different values of μ are also tabulated in Fig. 2. The stretch of material in the fracture zone $\Delta(\xi)$ is found to be very close to the analytical results

$$\Delta(\xi) = \sqrt{1-\xi} - \tfrac{1}{2}\xi \ln\left|\frac{1+\sqrt{1-\xi}}{1-\sqrt{1-\xi}}\right|, \tag{9}$$

obtained by Budiansky and Hutchinson (1978) for the special case $\mu = 0$.

Differentiation of eqn (6) with respect to ξ gives

$$f_1(\xi) = -\frac{d\Delta(\xi)}{d\xi} = \frac{\gamma\omega}{\sqrt{1-\xi}}\left\{\int_0^1 \frac{[1+\mu\Delta(\tau)]\sqrt{1-\tau}}{\tau-\xi}\,d\tau + \frac{1}{\sqrt{\omega}}\right\}. \tag{10}$$

It can be easily verified that $f_1(0) = \infty$ and $f_1(1) = 0$. The values of $-(d\Delta(\xi)/d\xi)$ at $K = K_{max}$ are shown in Fig. 3.

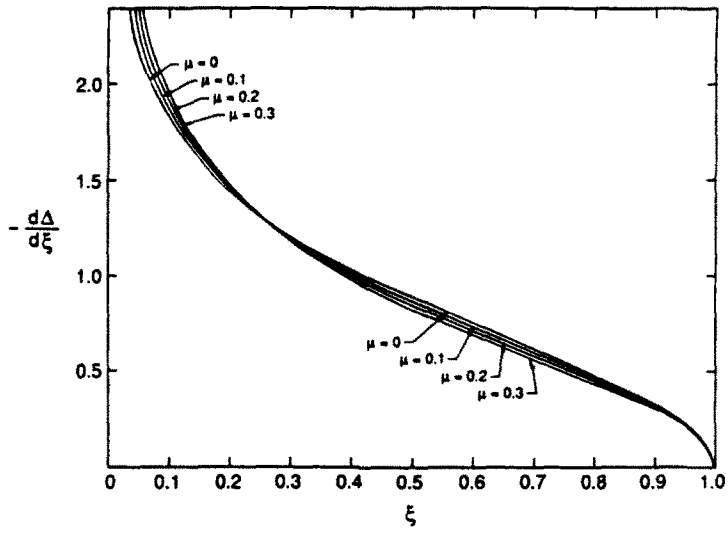

Fig. 3. Values of $-(d\Delta/d\xi)$ at $K = K_{max}$.

ANALYSIS OF GROWING FATIGUE CRACK

When the stress intensity factor K decreases from K_{max} to K_{cont}, the opened crack begins to close. For a further decrease in K, the closed region grows. When $K = K_{min} \geqslant 0$, the closed region is in $b \leqslant x \leqslant 0$, where $b < 0$. There is a reverse plastic zone within the fracture process zone in $0 \leqslant x \leqslant a$, as shown in Fig. 1. If $K_{min} = 0$, $b \to -\infty$. A mixed boundary value problem of this type can be analyzed by the complex variable technique.

Let the stretch in the fracture process zone at $K = K_{max}$ be denoted by δ_M, the stretch in the reverse plastic zone at $K = K_{min}$ be denoted by δ_m and the total residual plastic stretch at the crack tip be denoted by δ_R. When the value of K decreases to K_{min}, the plastic stretch in the elastically unloading zone $a \leqslant x \leqslant w$ has the same value as that under $K = K_{max}$ due to the rigid–plastic behavior of the model (Fig. 4).

Let us study the behavior of material points in the reverse plastic zone. During loading, the stress–stretch relation at any material point in the fracture process zone is shown by the line oaB in Fig. 5. When $K = K_{max}$, the stress and stretch at the material point reach maximum values at point B. During unloading, the stress in the reverse plastic zone decreases, but the stretch remains unchanged until the stress reaches point C. When the

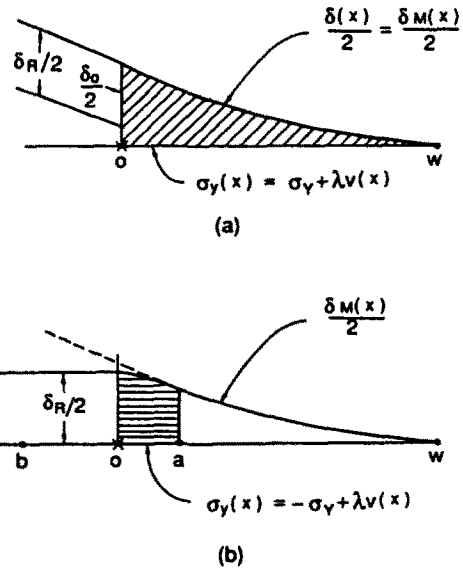

Fig. 4. Growing fatigue crack for (a) $K = K_{max}$, and (b) $K = K_{min} \geqslant 0$.

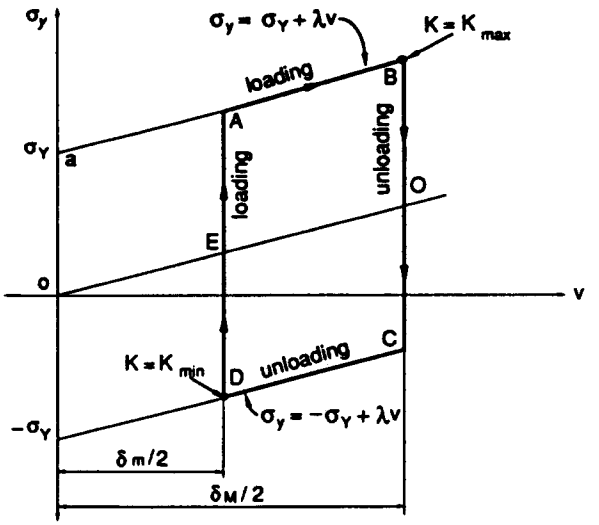

Fig. 5. Behavior of material points in the reverse plastic zone.

stress reaches point O, compression begins. As the stress reaches point C, the reverse plastic stretch occurs. If the unloading process continues, both the stress and stretch decrease. This procedure can be illustrated by the line CD in Fig. 5 with the relation

$$\sigma_y(x) = -\sigma_Y + \lambda v(x). \tag{11}$$

When $K = K_{\min}$, point D is reached. As the reloading process starts, the stress-stretch relation follows the line DA, where the stress increases but the stretch remains constant. When the stress reaches point A, the behavior of the material point in the reverse plastic zone will follow a path repeating the process described previously. Therefore, as the crack grows under a cycle of the periodic loading, the material points in the reverse plastic zone follow the loop ABCD. Obviously, on the line BC, the stretch is δ_M, while on the line AD, the stretch is δ_m. For the material point at the crack tip, $\delta_M = \delta_0$ and $\delta_m = \delta_R$. The behavior of material points in $(-\infty, 0)$ can always be described by the line AD, while the behavior of material points in $(\alpha, 1)$ can always be described by the line BC.

(1) *The case* $K_{min} = 0$

The state at $K_{\min} = 0$ can be analyzed by a boundary-value problem illustrated in Fig. 6. There are dislocations $\delta = \delta_R$ along $(-\infty, 0)$, compressive post-yielding stress in $(0, a)$ and a dislocation $\delta = \delta_M$ in (a, w). It is expected that $|\sigma_y| \leqslant |-\sigma_Y + \lambda\delta_R/2|$ in $(-\infty, 0)$, with σ_y vanishing monotonically as $x \to -\infty$. It is also anticipated that $-\sigma_Y + \lambda\delta_m(\alpha)/2 \leqslant \sigma_y \leqslant \sigma_Y$ in (a, w). These requirements will be shown later. Finally, the stresses are required to be bounded. These conditions suffice to determine values of δ_R and α.

In Budiansky and Hutchinson's (1978) work the complex Muskhelishvili potentials $\phi(z)$ and $\psi(z)$ were used for analysis. The condition for stress continuity across the x-axis permits an elimination of ψ. Thus stresses can be written in terms of $\phi(z)$, $\phi(\bar{z})$ and their derivatives by

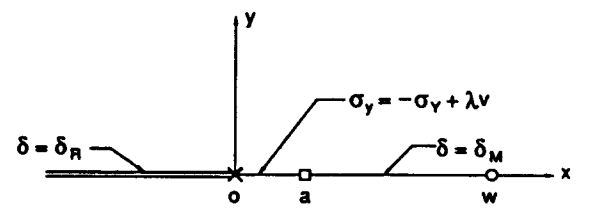

Fig. 6. Boundary values for $K = K_{\min} = 0$.

$$\sigma_x+\sigma_y = 2[\phi'(z)+\bar{\phi}'(\bar{z})], \tag{12}$$

$$\sigma_y-i\tau_{xy} = \phi'(z)+\bar{\phi}'(\bar{z})+(z-\bar{z})\bar{\phi}''(\bar{z}). \tag{13}$$

In the case of plane stress, the displacements u and v in the x- and y-directions satisfy

$$E\frac{\partial}{\partial x}(u+iv) = (3-\nu)\phi'(z)-(1+\nu)[\phi'(\bar{z})+(z-\bar{z})\bar{\phi}''(\bar{z})], \tag{14}$$

where ν is Poisson's ratio. On the x-axis, $z=\bar{z}$ and $\tau_{xy}=\partial u/\partial x=0$. Equations (13) and (14) are reduced to

$$\sigma_y = \phi'_+ + \phi'_- \tag{15}$$

and

$$\left(\frac{\partial v}{\partial x}\right)_+ - \left(\frac{\partial v}{\partial y}\right)_- = \frac{4}{iE}[\phi'_+ - \phi'_-]. \tag{16}$$

Let us define $\Phi=\phi'$. It follows from eqns (15) and (16) that the following conditions on Φ must hold along the x-axis:

$$\begin{aligned}
&\Phi_+ - \Phi_- = 0 && \text{for} \quad x<0,\\
&\Phi_+ + \Phi_- = -\sigma_Y + \lambda\delta_m/2 && 0<x<a,\\
&\Phi_+ - \Phi_- = \frac{iE}{4}\frac{\mathrm{d}\delta_M}{\mathrm{d}x} && a<x<w,\\
&\Phi_+ - \Phi_- = 0 && x>w.
\end{aligned} \tag{17}$$

By means of a technique similar to that given by Budiansky and Hutchinson (1978), the general solution for the problem of eqns (17) can be obtained:

$$\sqrt{z(z-a)}\Phi(z) = \frac{1}{2\pi}\int_0^a [-\sigma_Y+\lambda\delta_m(x)/2]\frac{\sqrt{x(a-x)}}{x-z}\,\mathrm{d}x + \frac{E}{8\pi}\int_a^w \frac{\sqrt{x(x-a)}}{x-z}\frac{\mathrm{d}\delta_M(x)}{\mathrm{d}x}\,\mathrm{d}x + \frac{E\delta_R}{8\pi}. \tag{18}$$

It is convenient to introduce the following dimensionless quantities:

$$\zeta = \frac{z}{w},\quad \alpha = \frac{a}{w},\quad F = \left(\frac{\pi^2}{\sigma_Y}\right)\Phi,\quad \Delta_M = \frac{\delta_M}{\delta_0},\quad \Delta_m = \frac{\delta_m}{\delta_0},\quad \Delta_R = \frac{\delta_R}{\delta_0}. \tag{19}$$

Equation (18) can be rewritten in a dimensionless form, as

$$\sqrt{\zeta(\zeta-\alpha)}F = \frac{\pi}{2}\int_0^\alpha [-1+\mu\Delta_m(\xi)]\frac{\sqrt{\xi(\alpha-\xi)}}{\xi-\zeta}\,\mathrm{d}\xi + \frac{1}{2\gamma\omega}\int_\alpha^1 \frac{\sqrt{\xi(\xi-\alpha)}}{\xi-\zeta}\frac{\mathrm{d}\Delta_M(\xi)}{\mathrm{d}\xi}\,\mathrm{d}\xi + \frac{\Delta_R}{2\gamma\omega}. \tag{20}$$

With the integral

$$\int_0^\alpha \frac{\sqrt{\xi(\alpha-\xi)}}{\xi-\zeta}\,d\xi = \pi\left[\sqrt{\zeta(\zeta-\alpha)}-\zeta+\frac{\alpha}{2}\right], \quad \text{for } \zeta \text{ out of } (0,\alpha), \tag{21}$$

and the requirement that the stresses σ_y are bounded at $\zeta = 0$ and α, eqn (20) yields

$$\frac{\pi^2\alpha}{4} = \frac{\pi\mu}{2}\int_0^\alpha \sqrt{\frac{\alpha-\xi}{\xi}}\,\Delta_m(\xi)\,d\xi + \frac{1}{2\gamma\omega}\int_\alpha^1 \sqrt{\frac{\xi-\alpha}{\xi}}\,\frac{d\Delta_M(\xi)}{d\xi}\,d\xi + \frac{\Delta_R}{2\gamma\omega} \tag{22}$$

and

$$-\frac{\pi^2\alpha}{4} = -\frac{\pi\mu}{2}\int_0^\alpha \sqrt{\frac{\xi}{\alpha-\xi}}\,\Delta_m(\xi)\,d\xi - \frac{1}{2\gamma\omega}\int_\alpha^1 \sqrt{\frac{\xi}{\alpha-\xi}}\,\frac{d\Delta_M(\xi)}{d\xi}\,d\xi + \frac{\Delta_R}{2\gamma\omega}. \tag{23}$$

Elimination of Δ_R from eqns (22) and (23) leads to

$$\frac{\pi^2}{2} = \frac{\pi}{2}\mu\int_0^\alpha \frac{\Delta_m(\xi)\,d\xi}{\sqrt{\xi(\alpha-\xi)}} + \frac{1}{2\gamma\omega}\int_\alpha^1 \frac{f_1(\xi)\,d\xi}{\sqrt{\xi(\xi-\alpha)}}, \tag{24}$$

where $f_1(\xi)$ is given by eqn (10).

With the use of dimensionless quantities in eqn (19), the discontinuity in the potential F across the x-axis can be written as

$$F_+ - F_- = \frac{\pi i}{\gamma\omega}\frac{d\Delta_m(\xi)}{d\xi} \quad \text{for} \quad 0 < \xi < \alpha. \tag{25}$$

From eqns (20) and (25), it is found that

$$\frac{\pi}{\gamma\omega}\sqrt{\xi(\alpha-\xi)}\,f_2(\xi) = \pi^2\left(\xi-\frac{\alpha}{2}\right) + \pi\mu\int_0^\alpha \frac{\sqrt{\tau(\alpha-\tau)}}{\tau-\xi}\,\Delta_m(\tau)\,d\tau - \frac{1}{\gamma\omega}\int_\alpha^1 \frac{\sqrt{\tau(\tau-\alpha)}}{\tau-\xi}\,f_1(\tau)\,d\tau + \frac{\Delta_R}{\gamma\omega}, \tag{26}$$

where $f_2(\xi)$ is defined by

$$f_2(\xi) = -\frac{d\Delta_m(\xi)}{d\xi}. \tag{27}$$

Elimination of Δ_R from eqns (22) and (26), with the use of eqn (24) gives

$$f_2(\xi) = \sqrt{\xi(\alpha-\xi)}\left[\mu\gamma\omega\int_0^\alpha \frac{\Delta_m(\tau)\,d\tau}{\sqrt{\tau(\alpha-\tau)}(\tau-\xi)} + \frac{1}{\pi}\int_\alpha^1 \frac{f_1(\tau)\,d\tau}{\sqrt{\tau(\tau-\alpha)}(\tau-\xi)}\right]. \tag{28}$$

Equations (24) and (28) are the governing equations of the problem.

It can be shown from eqn (28) that

$$\lim_{\xi\to 0} f_2(\xi) = 0, \tag{29}$$

and

$$\lim_{\xi\to\alpha} f_2(\xi) = f_1(\alpha). \tag{30}$$

Hence, the stretch slope at $\xi = \alpha$ is continuous.

In the contact region $(-\infty, 0)$, the boundary value problem becomes

$$F_+ + F_- = \pi^2\left(\frac{\sigma_y}{\sigma_Y}\right) \quad \text{for} \quad \xi < 0. \tag{31}$$

Therefore, use of eqn (20) and elimination of Δ_R from eqn (22) yield

$$\frac{\sigma_y}{\sigma_Y} = -1 + \frac{|\xi|}{\alpha+|\xi|}\left[1 + \frac{\mu}{\pi}\int_0^\alpha \frac{\Delta_m(\tau)}{\tau+|\xi|}\sqrt{\frac{\alpha-\tau}{\tau}}\,d\tau - \frac{1}{\pi^2\gamma\omega}\int_\alpha^1 \frac{f_1(\tau)}{\tau+|\xi|}\sqrt{\frac{\tau-\alpha}{\tau}}\,d\tau\right] \quad \text{for} \quad \xi < 0. \tag{32}$$

It can be shown through eqn (32) that

$$\sigma_y(0)/\sigma_Y = -1 + \mu\Delta_m(0). \tag{33}$$

Therefore, the stress at $\xi = 0$ is continuous.

It can be verified easily by eqn (32) that

$$\lim_{\xi\to-\infty}\left(\frac{\sigma_y}{\sigma_Y}\right) = 0. \tag{34}$$

The numerical calculation shows that the magnitude of σ_y from $\xi = 0$ to $\xi = -\infty$ decreases monotonically. Hence, the contact stress in $(-\infty, 0)$ satisifes the condition $0 > \sigma_y/\sigma_Y \geqslant -1 + \mu\Delta_R$, or $|\sigma_y| \leqslant |-\sigma_Y + \lambda\delta_R/2|$.

With the elimination of Δ_R from eqns (20) and (22), the potential function on the real axis with $\alpha < \xi < 1$ can be written as

$$F = -\frac{\pi^2}{2}\left(1 - \sqrt{\frac{\xi-\alpha}{\xi}}\right) - \frac{\pi}{2}\sqrt{\frac{\xi-\alpha}{\xi}}\,\mu\int_0^\alpha \sqrt{\frac{\tau}{\alpha-\tau}}\,\frac{1}{\tau-\xi}\,\Delta_m(\tau)\,d\tau$$
$$- \frac{1}{2\gamma\omega}\sqrt{\frac{\xi-\alpha}{\xi}}\int_\alpha^1 \sqrt{\frac{\tau}{\tau-\alpha}}\,\frac{1}{\tau-\xi}\,f_1(\tau)\,d\tau \quad \text{for} \quad \alpha < \xi < 1. \tag{35}$$

Thus, in the elastic unloading zone $(\alpha, 1)$, the stress can be determined by

$$\frac{\sigma_y}{\sigma_Y} = \frac{1}{\pi^2}(F_+ + F_-)$$
$$= -\left(1 - \sqrt{\frac{\xi-\alpha}{\xi}}\right) - \frac{1}{\pi}\sqrt{\frac{\xi-\alpha}{\xi}}\,\mu\int_0^\alpha \sqrt{\frac{\tau}{\alpha-\tau}}\,\frac{1}{\tau-\xi}\,\Delta_m(\tau)\,d\tau$$
$$- \frac{1}{\gamma\omega\pi^2}\sqrt{\frac{\xi-\alpha}{\xi}}\int_\alpha^1 \sqrt{\frac{\tau}{\tau-\alpha}}\,\frac{1}{\tau-\xi}\,f_1(\tau)\,d\tau \quad \text{for} \quad \alpha < \xi \leqslant 1. \tag{36}$$

It can be verified that

$$\sigma_y(\alpha)/\sigma_Y = \lim_{\xi\to\alpha}\left\{-\left(1 - \sqrt{\frac{\xi-\alpha}{\xi}}\right) - \frac{1}{\pi}\sqrt{\frac{\xi-\alpha}{\tau}}\,\mu\int_0^\alpha \sqrt{\frac{\tau}{\alpha-\tau}}\,\frac{\Delta_m(\tau)}{\tau-\xi}\,d\tau\right.$$
$$\left. - \frac{1}{\gamma\omega\pi^2}\sqrt{\frac{\xi-\alpha}{\xi}}\int_\alpha^1 \sqrt{\frac{\tau}{\tau-\alpha}}\,\frac{1}{\tau-\xi}\,f_1(\tau)\,d\tau\right\} = -1 + \mu\Delta_m(\alpha). \tag{37}$$

Therefore, the stress at $\xi = \alpha$ is continuous.

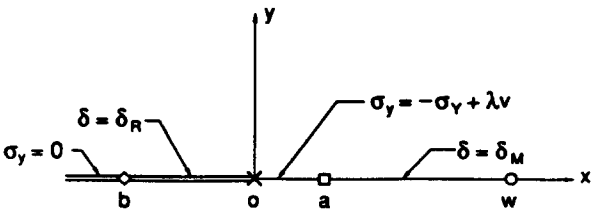

Fig. 7. Boundary values for $K = K_{min} > 0$.

(ii) *The case* $K_{min} > 0$

The boundary value problem at $K_{min} > 0$ is illustrated in Fig. 7. It is found that all of the boundary conditions and the behavior of material points in different regions are the same as those in the case of $K_{min} = 0$, except that there is a contact region $(b, 0)$ on the negative real axis. With an introduction of the dimensionless quantities in eqn (19), the boundary conditions can be written as

$$\begin{aligned}
&F_+ + F_- = 0 && \text{for} \quad \xi < \beta,\\
&F_+ - F_- = 0 && \beta < \xi < 0,\\
&F_+ + F_- = \pi^2[-1 + \mu\Delta_m(\xi)] && 0 < \xi < \alpha,\\
&F_+ - F_- = \frac{\pi i}{\gamma\omega}\frac{\mathrm{d}\delta_M}{\mathrm{d}\xi} && \alpha < \xi < 1,\\
&F_+ - F_- = 0 && \xi > 1,
\end{aligned} \tag{38}$$

where $\beta = b/w$. By means of the technique used by Budiansky and Hutchinson (1978), the solution of the problem can be obtained, i.e.

$$\sqrt{(\zeta-\beta)\zeta(\zeta-\alpha)}F(\zeta) = \frac{\pi}{2}\int_0^\alpha \frac{[-1+\mu\Delta_m(\xi)]\sqrt{(\xi-\beta)\xi(\alpha-\xi)}}{\xi-\zeta}\,\mathrm{d}\xi + \frac{1}{2\gamma\omega}\int_\alpha^1 \frac{\sqrt{(\xi-\beta)\xi(\xi-\alpha)}}{\xi-\zeta}\frac{\mathrm{d}\Delta_M(\xi)}{\mathrm{d}\xi}\,\mathrm{d}\xi + \frac{\pi}{2\sqrt{\omega}}(A+R\zeta). \tag{39}$$

The boundness of the stress σ_y at $\zeta = \beta$, 0 and α leads to

$$\frac{\pi}{2}\int_0^\alpha \frac{-1+\mu\Delta_m(\xi)}{\sqrt{(\xi-\beta)\xi(\alpha-\xi)}}\,\mathrm{d}\xi + \frac{1}{2\gamma\omega}\int_\alpha^1 \frac{f_1(\xi)\,\mathrm{d}\xi}{\sqrt{(\xi-\beta)\xi(\xi-\alpha)}} = 0, \tag{40}$$

$$\frac{\pi A}{\sqrt{\omega}} = -\pi\int_0^\alpha [-1+\mu\Delta_m(\xi)]\sqrt{\frac{(\xi-\beta)(\alpha-\xi)}{\xi}}\,\mathrm{d}\xi + \frac{1}{\gamma\omega}\int_\alpha^1 f_1(\xi)\sqrt{\frac{(\xi-\beta)(\xi-\alpha)}{\xi}}\,\mathrm{d}\xi, \tag{41}$$

and

$$\frac{\pi R}{\sqrt{\omega}} = -\pi\int_0^\alpha [-1+\mu\Delta_m(\xi)]\sqrt{\frac{\alpha-\xi}{(\xi-\beta)\xi}}\,\mathrm{d}\xi + \frac{1}{\gamma\omega}\int_\alpha^1 \sqrt{\frac{\xi-\alpha}{(\xi-\beta)\xi}}f_1(\xi)\,\mathrm{d}\xi. \tag{42}$$

With the use of

$$F_+ - F_- = \frac{\pi i}{\gamma\omega}\frac{d\Delta_m}{d\xi} = -\frac{\pi i}{\gamma\omega} f_2(\xi) \quad \text{for} \quad 0 < \xi < \alpha, \tag{43}$$

eqn (39) yields

$$f_2(\xi) = \sqrt{\frac{(\xi-\beta)\xi}{\alpha-\xi}}\left\{\gamma\omega\int_0^\alpha \frac{-1+\mu\Delta_m(\tau)}{\tau-\xi}\sqrt{\frac{\alpha-\tau}{(\tau-\beta)\tau}}\,d\tau - \frac{1}{\pi}\int_\alpha^1 \frac{f_1(\tau)}{\tau-\xi}\sqrt{\frac{\tau-\alpha}{(\tau-\beta)\tau}}\,d\tau\right\} \quad 0 < \xi < \alpha. \tag{44}$$

Equations (40) and (44) are the governing equations of the problem.

It can be shown that

$$\lim_{\xi\to 0} f_2(\xi) = 0 \tag{45}$$

and

$$\lim_{\xi\to\alpha} f_2(\xi) = f_1(\alpha). \tag{46}$$

Thus, the stretch slope is continuous at $\xi = 0$ and $\xi = \alpha$.

In the region $(\beta, 0)$, the boundary value is

$$F_+ + F_- = \pi^2\frac{\sigma_y}{\sigma_Y} \quad \text{for} \quad \beta < \xi < 0. \tag{47}$$

With the elimination of A and R from eqns (39), (41) and (42), eqn (47) leads to

$$\frac{\sigma_y(\xi)}{\sigma_Y} = \sqrt{\frac{|\xi|(\xi-\beta)}{\alpha+|\xi|}}\left\{\frac{1}{\pi}\int_0^\alpha \frac{-1+\mu\Delta_m(\xi)}{\tau+|\xi|}\sqrt{\frac{\alpha-\tau}{\tau(\tau-\beta)}}\,d\tau - \frac{1}{\pi^2\gamma\omega}\int_\alpha^1 \frac{1}{\tau+|\xi|}\sqrt{\frac{\tau-\alpha}{\tau(\tau-\beta)}}\,f_1(\tau)\,d\tau\right\} \quad \beta < \xi < 0. \tag{48}$$

It can be shown that

$$\sigma_y(\beta) = 0, \tag{49}$$

$$\sigma_y(0)/\sigma_Y = -1+\mu\Delta_m(0). \tag{50}$$

Therefore, the stresses at $\xi = \beta$ and $\xi = 0$ are continuous.

In the elastic unloading zone $(\alpha, 1)$, eqns (47) and (48) still hold. With the elimination of A and R from eqns (39), (41) and (42), eqn (47) also yields

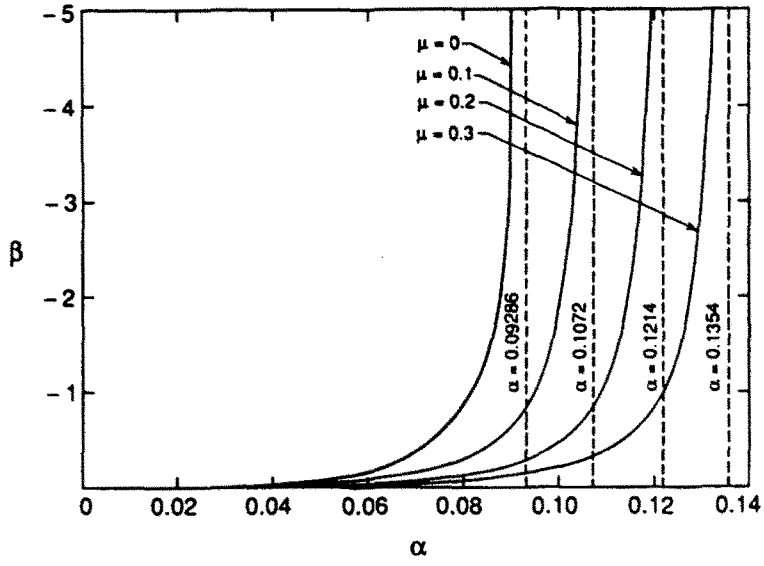

Fig. 8. Relations between β and α.

$$\pi^2 \frac{\sigma_y}{\sigma_Y} = F_+ + F_-$$

$$= -\sqrt{\frac{\xi(\xi-\beta)}{\xi-\alpha}} \left\{ \pi \int_0^{\alpha} [-1+\mu\Delta_m(\tau)] \sqrt{\frac{\alpha-\tau}{\tau(\tau-\beta)}} \frac{d\tau}{\tau-\xi} \right.$$

$$\left. - \frac{1}{\gamma\omega} \int_{\alpha}^{1} f_1(\tau) \sqrt{\frac{\tau-\alpha}{(\tau-\beta)\tau}} \frac{d\tau}{\tau-\xi} \right\} \quad \text{for } \alpha < \xi \leqslant 1. \tag{51}$$

It can be shown from eqn (51) that

$$\sigma_y(\alpha)/\sigma_Y = -1+\mu\Delta_m(\alpha). \tag{52}$$

Thus, the stress at $\xi = \alpha$ is continuous.

(iii) *Numerical results*

Equations (28) and (44) can be integrated by means of the Runge–Kutta method. Here the range of integration will start at $\xi = \alpha$ with negative increments of ξ and will terminate at $\xi = 0$. The initial values are $f_2(\alpha) = f_1(\alpha)$ and $\Delta_m(\alpha) = \Delta_M(\alpha)$. It is found that the continuity condition $f_2(0) \equiv 0$ is always satisfied no matter what value α has. Therefore the values of α have to be determined by eqns (24) and (40).

Unfortunately, the value of $f_2(\xi)$ at any point in $(0, \alpha)$ depends on the value of $\Delta_m(\xi)$ in the entire interval. Therefore, an iterative process is necessary for the determination of $\Delta_m(\xi)$. First of all, an initially tried function for $\Delta_m(\xi)$ can be assumed. Equations (28) and (44) can then be solved for the new function, $\Delta_m(\xi)$. This iterative process continues until a prescribed tolerance is reached. This method is found to be so effective that the absolute tolerance of $\Delta_m(\xi)$ can be less than 10^{-5} after three iterations. Another iteration is required for determining α and β. In the case of $K_{min} > 0$, the values of R can then be found numerically through eqn (42).

In eqns (28) and (44), some integrands are singular or ill-behaved at $\tau = 0$, α and/or ξ. Special techniques such as change of variables, piecewise parabolic interpolation, Simpson's rule with unequal spacings, etc. must be employed for evaluation of integrals.

In Fig. 8, the relations between α and β for different values of μ are shown. The vertical dashed lines denote the asymptotic lines of the curves as $\beta \to -\infty$. The values of α as shown on the dashed lines correspond to the case of $R = 0$. The case $\mu = 0$ agrees with the results

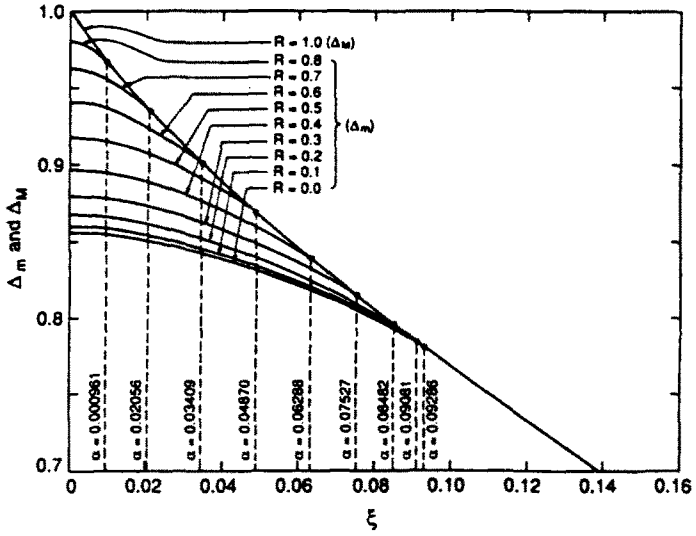

Fig. 9. Stretch in the reverse plastic zone ($\mu = 0$).

obtained by Budiansky and Hutchinson (1978). All curves terminate at the origin $\alpha = 0$ and $\beta = 0$.

Figures 9–12 show the plastic stretch Δ_m in the reverse plastic zone for different values of μ and R. The solid circles denote the boundaries of the reverse plastic zone for different values of R. Dashed vertical lines pass through the solid circles. The corresponding values of α are also indicated on these lines. It can be seen that the stretch slope is continuous at $\xi = \alpha$ and $\xi = 0$ and the length of the reverse plastic zone decreases as the value of R increases.

SPEED OF FATIGUE CRACK PROPAGATION

For any infinitesimal material element, the total accumulative plastic work (TAPW) is the sum of the following parts: (i) the crack opening plastic work due to the propagation of the crack; and (ii) the accumulative oscillation plastic work induced by the oscillatory motion of the boundary of the reverse plastic zone in $0 \leqslant x \leqslant a$. The ratio of the TAPW and the infinitesimal length of the element is regarded as the "density of the total accumulative plastic work" applied to the material point. The criterion of TAPW states that failure at a material point occurs as the density of TAPW of the material point reaches a certain critical value W_c. For fatigue crack propagation, the material point is at the crack tip.

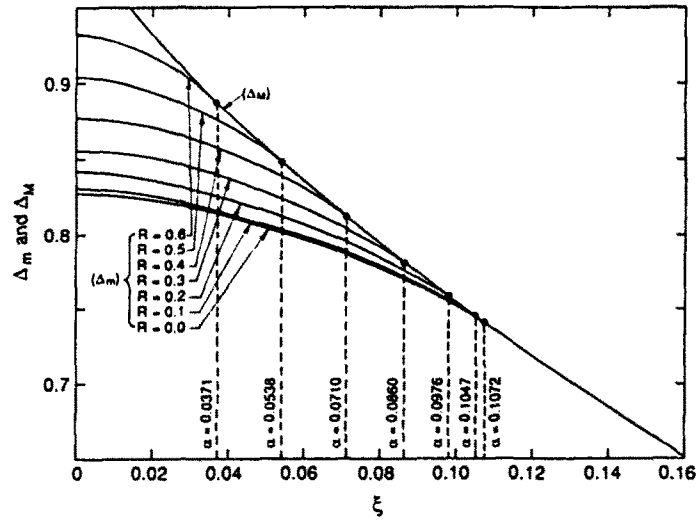

Fig. 10. Stretch in the reverse plastic zone ($\mu = 0.1$).

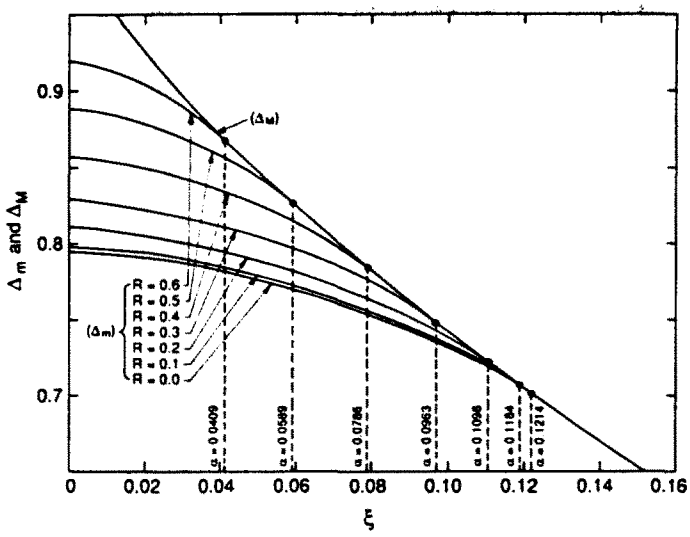

Fig. 11. Stretch in the reverse plastic zone ($\mu = 0.2$).

The magnitude of the density of crack opening plastic work at a material point increases gradually as the crack tip propagates toward the material point. This magnitude attains its maximum value when the stretched length of material in the fracture process zone reaches a maximum. It is

$$W_1 = \int_0^{\delta_0} \left(\sigma_Y + \lambda \frac{\delta}{2}\right) \mathrm{d}\delta. \tag{53}$$

With the use of dimensionless quantities, the density of crack opening plastic work at crack tip W_1 can be expressed as

$$\begin{aligned} W_1 &= \sigma_Y \delta_0 \int_0^1 (1 + \mu \Delta_M)\, \mathrm{d}\Delta_M \\ &= \sigma_Y \delta_0 \left(1 + \frac{\mu}{2}\right). \end{aligned} \tag{54}$$

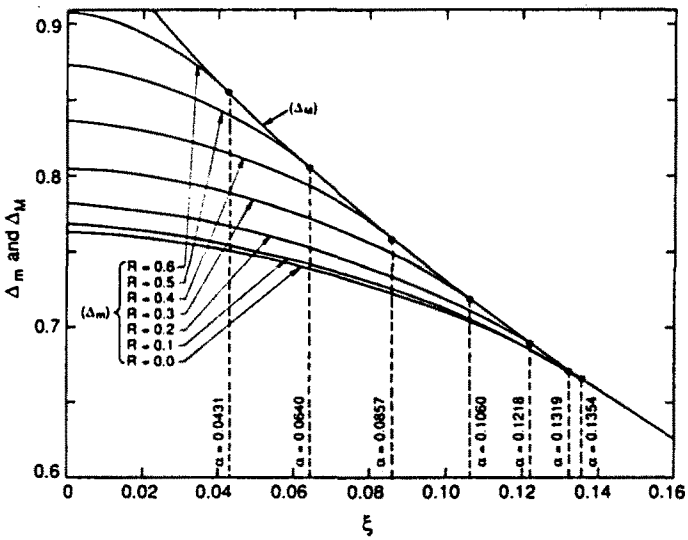

Fig. 12. Stretch in the reverse plastic zone ($\mu = 0.3$).

The oscillatory plastic work at a material point is the accumulation of the plastic work applied to the material point as it moves backward through the entire reverse plastic zone. For each cycle of oscillation, the crack tip propagates forward by a distance dl/dN. Hence, the plastic work applied to the material point within $0 \leqslant x \leqslant a$ through one cycle of oscillation can be approximated by

$$dW_2 = 2\frac{\sigma_Y}{\dfrac{dl}{dN}}[\delta_M(x) - \delta_m(x)]\,dx, \tag{55}$$

where the factor two stems from the unloading and reloading process in each cycle. The density of the total oscillatory plastic work at the crack tip is therefore

$$W_2 = 2\frac{\sigma_Y}{\dfrac{dl}{dN}}\int_0^a [\delta_M(x) - \delta(x)]\,dx. \tag{56}$$

Note that W_2 is independent of λ, the coefficient of linear work-hardening, because the hardening effect will be cancelled in the loading and unloading process. In fact, the quantity dW_2 in eqn (55) is the magnitude of the area of the loop ABCD as shown in Fig. 5.

The criterion of TAPW requires

$$W_1 + W_2 = W_c. \tag{57}$$

Substitution of eqns (54) and (56) into eqn (57) leads to

$$\frac{dl}{dN} = \frac{2\sigma_Y}{W_c - \sigma_Y\delta_M(0)\left(1+\dfrac{\mu}{2}\right)}\int_0^a [\delta_M(x) - \delta_m(x)]\,dx. \tag{58}$$

Use of dimensionless quantities transforms eqn (58) into

$$\frac{dl}{dN} = G_1(K_{max})F_2(R), \tag{59}$$

where

$$F_2(R) = \int_0^z [\Delta_M(\xi) - \Delta(\xi)]\,d\xi, \tag{60}$$

$$G_1(K_{max}) = \frac{\pi K_{max}^2\delta_0\omega}{\left[W_c - \sigma_Y\delta_0\left(1+\dfrac{\mu}{2}\right)\right]\sigma_Y}. \tag{61}$$

The quantity W_c in eqn (61) can be expressed as

$$W_c = \frac{K_f^2}{E}, \tag{62}$$

where K_f is called the fatigue fracture toughness. When $K_{max} = K_{min} = K_f$, the value of W_2 is required to be zero. Thus

$$W_1 = \sigma_Y \delta_f \left(1 + \frac{\mu_f}{2}\right) = W_c, \tag{63}$$

where δ_f and μ_f are defined by

$$\delta_f = \delta_0|_{K=K_f} = \frac{2K_f^2}{\sigma_Y \gamma_f E} \tag{64}$$

and

$$\mu_f = \mu|_{K=K_f} = \frac{\delta_f}{2\sigma_Y}\lambda, \tag{65}$$

where γ_f is defined by

$$\gamma_f = \gamma|_{K=K_f}. \tag{66}$$

From eqn (63), eqn (61) becomes

$$G_1(K_{max}) = \frac{\pi K_{max}^2 \delta_0 \omega}{\left[\delta_f\left(1 + \frac{\mu_f}{2}\right) - \delta_0\left(1 + \frac{\mu}{2}\right)\right]\sigma_Y^2}. \tag{67}$$

With the introduction of the following quantities:

$$d = \frac{\delta_0}{\delta_f}, \tag{68}$$

$$m = \frac{1 + \frac{\mu}{2}}{1 + \frac{\mu_f}{2}}, \tag{69}$$

$$k_m = \frac{K_{max}}{K_f}, \tag{70}$$

$$F_1(k_m) = \frac{k_m^2 d}{1 - md} = \frac{k_m^4}{\frac{\gamma}{\gamma_f} - mk_m^2} \tag{71}$$

and

$$\bar{l} = \frac{\sigma_Y^2(1 + \mu_f/2)}{\pi K_f^2 \omega} l, \tag{72}$$

the dimensionless speed of fatigue crack growth is then obtained from equations (59) and (67) as

$$\frac{d\bar{l}}{dN} = F_1(k_m)F_2(R). \tag{73}$$

It is seen that $d\bar{l}/dN$ approaches infinity as K_{max} approaches K_f. Let $\Delta k = (K_{max} - K_{min})/K_f$. Equation (73) can also be expressd in terms of Δk and R as

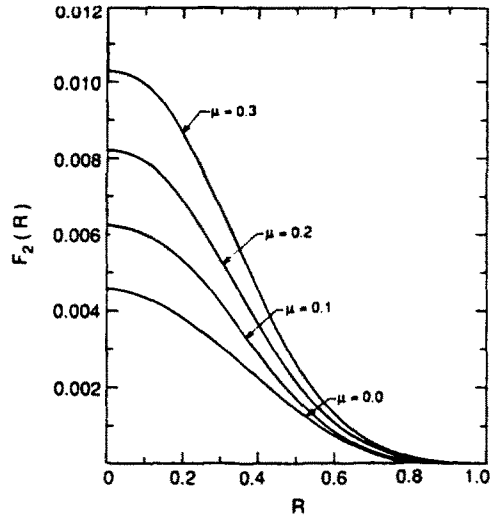

Fig. 13. $F_2(R)$ curves.

$$\frac{dl}{dN} = \frac{(\Delta K)^4}{\frac{\gamma}{\gamma_f}(1-R)^2 - m(\Delta k)^2} \frac{F_2(R)}{(1-R)^2}. \tag{74}$$

When $k_m \ll 1$, the fatigue crack speed can be approximated by

$$\frac{dl}{dN} = F_3(r)(\Delta k)^4, \tag{75}$$

where

$$F_3(R) = \frac{F_2(R)}{\frac{\gamma}{\gamma_f}(1-R)^4}, \tag{76}$$

when $k_m \ll 1$, γ/γ_f approaches a constant. Hence, the fourth power law for the steady speed of fatigue crack growth is obtained.

Figure 13 shows the relation between $F_2(R)$ and R. When $R = 1$, the value of $F_2(R)$ vanishes. When $R = 0$, the slopes of the curves are equal to zero. This phenomenon is caused by the constant value of the oscillatory plastic work for $R < 0$, which is equal to the value of $F_2(0)$ for $R = 0$. This problem will be discussed later.

For linear work-hardening materials, the relations of the parameters μ, γ, ω with respect to material constants E, σ_Y, K_f and loading parameters K_{max}, R, etc. have no concise analytical forms. However, their numerical relations can be found empirically. From the table shown in Fig. 2, it is found that the relation between γ and μ is nearly linear. Therefore, $\gamma(\mu)$ can be written as

$$\gamma(\mu) = \gamma(0) + \frac{1}{0.3}[\gamma(0.3) - \gamma(0)]\mu = 2 + 0.992\mu. \tag{77}$$

From eqn (5), another relation between γ and μ is found to be

$$\gamma = \frac{K_{max}^2 \lambda}{\mu \sigma_Y^2 E}. \tag{78}$$

Combination of eqns (77) and (78) leads to an equation for solving μ:

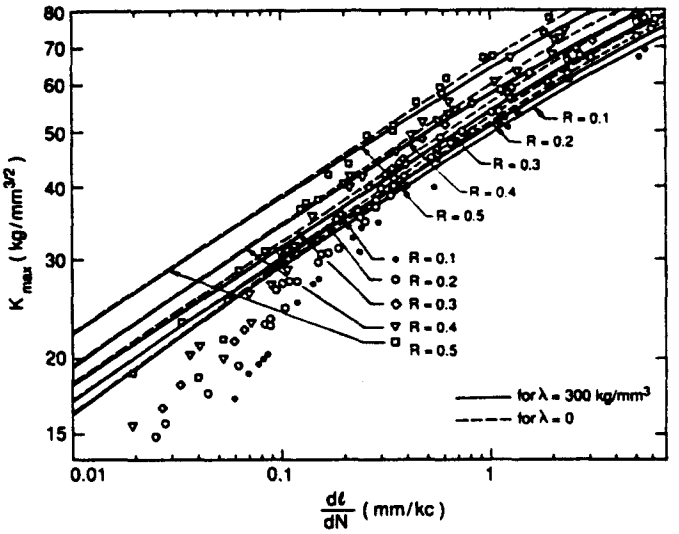

Fig. 14. Comparison of the theoretical fatigue crack speeds with the experimental values for 2024-T3 alloy, $\sigma_Y = 40$ kg mm^{-2} and $K_f = 130$ kg mm$^{-3/2}$.

$$0.992\mu^2 + 2\mu - \frac{K_{max}^2 \lambda}{\sigma_Y^2 E} = 0. \tag{79}$$

After μ is solved, γ and ω can be determined by the interpolation according to the numerical relation as shown in the table of Fig. 2. The value of δ_0 can then be determined by eqn (5). In the special case of $K_{max} = K_f$, this method determines the values of μ_f, γ_f, ω_f and δ_f. With eqns (68)–(71), $F_1(k_m)$ can be found. Function $F_2(R)$ can be determined numerically by using Fig. 13. From eqns (72) and (73) the speed of fatigue crack propagation can then be determined.

As an example, the value of dl/dN is calculated with respect to K_{max}. Our theoretical speeds of fatigue crack growth are compared with the experimental data given by Broek (1981) for 2024-T3 aluminum alloy. Material constants are $\sigma_Y = 40$ kg mm^{-2}, $K_f = 130$ kg mm$^{-3/2}$, $E = 7000$ kg mm^{-2}. The value of λ is selected to be 300 kg mm^{-3}. The relations between dl/dN and K_{max} are shown in Fig. 14, where the dashed lines denote the results for $\lambda = 0$ corresponding to the case of no work-hardening. The solid lines denote the results for $\lambda = 300$ kg mm^{-3}. It is seen that the solid lines agree with experimental data better than the dotted lines as long as the value of K_{max} is not too small. When K_{max} decreases, all solid lines approach the corresponding dashed lines asymptotically.

Broek (1981) observed from the fatigue test of aluminum alloy that the fracture surface could change from a tensile mode to a shear mode during the growth of a fatigue crack. A state of plane strain is associated with the tensile mode and a state of plane stress is associated with the shear mode. Since our theory is based on the assumption of plane stress, the theoretical results given in this paper check well with the experimental data corresponding to sufficiently high values of K_{max} where the fracture mode is governed by the state of plane stress.

DISCUSSION AND CONCLUSION

Rice (1967) pointed out that for most metals, the experimental values of the exponential constant in the power law for the speed of steady fatigue crack growth lie between two and four, depending on the portion of dl/dN versus Δk curve. However, Weertman (1966) found that the theoretical prediction based on the TAPW criterion and the Dugdale model always leads to Paris' fourth power law of fatigue crack speed at low values of K_{max}. Huang and Li (1989) proposed that the theory can be improved by considering a model with a

complicated constitutive relation for the deformation of the fracture process zone. Work-hardening behavior of material is a possible constitutive relation for the improvement.

The authors of this paper employed a modified Dugdale model by including the effects of either the cyclic softening or Baushinger effect. They found that these effects merely lead to a shift of the dl/dN versus K_{max} curves in the vertical or horizontal directions. The modified Dugdale model with linear hardening effect, as employed in this analysis, can alter the shape of the dl/dN versus K_{max} curves for sufficiently large values of K_{max}. When the value of k_m decreases, the dl/dN versus K_{max} curves based on our model approach asymptotically those based on the Dugdale model with an ideally plastic constitutive relation of the fracture process zone. A more complicated and realistic constitutive relation for the material behavior in the fracture process zone may be used for study. However, it is found that the expression of the speed of fatigue crack growth will still retain a form as given by eqn (74). Therefore, the fourth power law of fatigue crack speed at low values of K_{max} seems to be inevitable as long as the Dugdale model for the active plastic zone and the criterion of total accumulative plastic work are employed.

In order to estimate the width of the active plastic zone, let us consider the plastic zone of finite width and employ the following constitutive relation for loading

$$\sigma_y = \sigma_Y + E_1 \varepsilon_y, \tag{80}$$

where E_1 is the tangent modulus. For linear hardening material, the value of E_1 is a constant. Since ε_y is the normal strain in the vertical direction in the plastic zone of finite width, it may be expressed approximately by

$$\varepsilon_y = \frac{\delta}{W_p}, \tag{81}$$

where W_p is the width of the plastic zone, and δ is the plastic stretch obtained from the Dugdale model in which the width of the plastic zone is regarded as zero. An equation similar to the combination of eqns (80) and (81) was presented by Rice (1968). Hahn and Rosenfield (1965) noted that some metals actually reveal a narrow slit-like plastic zone, of width approximately equal to plate thickness ahead of the crack when the zone is long in comparison to the thickness of the plate. By comparison of eqns (80) and (81) with eqn (1), it is found that

$$\lambda = \frac{2E_1}{W_p}. \tag{82}$$

For 2024-T3 aluminum alloy, $E_1 = 700$ kg mm^{-2}. For a given value of $\lambda = 300$ kg mm^{-3}, the width of the active plastic zone is found by eqn (82) to be 4.67 mm, which is in the same order as the thickness of the plate used for fatigue experiments.

The authors of this paper also considered the problem of fatigue crack propagation under the condition $R < 0$. The reverse plastic zone exists on the negative x-axis. The contact region extends to $-\infty$ with a constant residual stretch δ_R attached to the crack surface. They considered an additional reverse plastic zone along the negative x-axis with different sizes, and used the J-integral to estimate the minimum stress intensity factor K_{min}. However, they always obtained small positive values for K_{min}. This implies that the negative value of R only produces a nominal negative value for K_{min}. In reality, no negative K_{min} exists. The smallest value of R is actually zero as a result of the contact of the crack surface under compressive remote loading. Hence, the case of $R < 0$ can be replaced by the case of $R = 0$. This point of view is in agreement with that proposed by Hertzberg (1983).

In conclusion, this work applies the complex variable technique for the analysis of the fatigue crack propagation problem, based on the model of strip yielding with a rigid–plastic linear work-hardening constitutive relation for material in the fracture process zone. The boundary value problem is governed by a set of integro-differential equations which can be

solved numerically. The theoretical results obtained here check well with experimental data for sufficiently large values of K_{max}. It indicates that the work-hardening characteristics of material in the fracture process zone plays an important role in fatigue crack propagation. For small values of K_{max}, the theoretical results approach, asymptotically, the fourth power law which provides the fatigue crack growth rate always smaller than the experimental value.

REFERENCES

Broek, D. (1981). *Elementary Engineering Fracture Mechanics*, 3rd revised edn, pp. 254–258. Martinus Nijhoff, The Hague.

Budiansky, B. and Hutchinson, J. W. (1978). Analysis of closure in fatigue crack growth. *J. Appl. Mech.* **45**, 267–276.

Elber, W. (1970). Fatigue crack closure under cyclic tension. *Engng Fract. Mech.* **2**, 37–45.

Hahn, G. T. and Rosenfield, A. R. (1965). Local yielding and extension of a crack under plane stress. *Acta Metallurgica* **13**(3), 293–306.

Hertzberg, R. W. (1983). *Deformation and Fracture Mechanics of Engineering Materials*, 2nd edn, p. 544. John Wiley, NY.

Huang, N. C. (1988). Fatigue crack growth under anti-plane shear mode deformation. *Theoret. Appl. Fract. Mech.* **10**, 231–239.

Huang, N. C. and Li, Y. C. (1989). Steady fatigue crack growth under tensile load. *Engng Fract. Mech.* **33**(3), 477–481.

Lardner, B. A. (1968). A dislocation model for fatigue crack growth in metals. *Phil. Mag.* **17**, 71–82.

Liu, H. W. (1961). Crack propagation in thin metal sheets under repeated loading. Transactions, American Society of Mechanical Engineers. Series D. *J. Basic Engng* **83**, 23–31.

McClintock, F. A. (1963). On the plasticity of the growth of fatigue cracks. In *Fracture of Solids* (Edited by D. C. Drucker and J. J. Gilman), pp. 103–118. John Wiley, NY.

Newman, J. C. Jr (1976). A finite-element analysis of fatigue crack closure. *Mechanics of Crack Growth*. ASTM STP 590, pp. 281–301.

Paris, P. C. and Erdogan, F. (1963). A critical analysis of crack propagation laws. *J. Basic Engng* **85**, 528–534.

Rice, J. R. (1965). Plastic yielding at a crack tip. *Proc. International Conf. of Fracture*, pp. 283–308. Sendi, Japan.

Rice, J. R. (1967). Mechanics of crack tip deformation and extension by fatigue. *Fracture Crack Propagation*. ASTM STP 415, American Society for Testing and Materials, pp. 247–309.

Rice, J. R. (1968). A path independent integral and the approximate analysis of strain concentration by notches and cracks. *J. Appl. Mech.* **35**, 379–386.

Weertman, J. (1966). Rate of growth of fatigue cracks as calculated from the theory of infinitesimal dislocation distributed on a plane. *Int. J. Fract. Mech.* **2**, 460–467.